Turbulence, Heat and Mass Transfer 10

Pressure-velocity coupling on unstructured collocated grids: reconciling stability and energy-conservation

D. Santos, F.X. Trias, J.A. Hopman, C.D. Pérez-Segarra
Heat and Mass Transfer Technological Center (CTTC), Technical University of Catalonia, C/Colom 11, 08222 Terrassa (Barcelona), Spain, daniel.santos.serrano@upc.edu, francesc.xavier.trias@upc.edu, jannes.hopman@upc.edu, cdavid.perez.segarra@upc.edu

Abstract – In this work, an energy-preserving unconditionally stable fractional step method on collocated unstructured grids is presented. Its formulation is based on preserving the underlying symmetries of the differential operators. This formulation was proven to be unconditionally stable even for highly distorted meshes [1, 2]. Conservation of (global) kinetic energy is also a key feature in simulations. Within this context, a canonical case is tested, a differentially heated cavity, in order to show that the (artificial) kinetic energy error introduced by the pressure is negative and small compared with the physical dissipation. Furthermore, a stability and accuracy comparison is done for the three classical ways of interpolating the pressure gradient: linear interpolation, mid-point interpolation and volumetric interpolation.

1. Introduction

General purpose CFD codes such as OpenFOAM or ANSYS-Fluent use a finite-volume (stencil) discretization over unstructured meshes and a collocated formulation to solve the Navier-Stokes equations. The stencil formulations solve the discretised equations using an algorithm that calculates the desired values cell by cell. Alternatively, algebraic formulations keep them in matrix-vector form, and use these matrices and vectors to calculate the desired quantities.

A collocated fully-conservative algebraic symmetry-preserving formulation of incompressible Navier-Stokes equations was proposed by Trias et al.[3]. Assuming n control volumes and m faces:

$$\Omega\frac{d\mathbf{u}_c}{dt}+\mathbf{C}(\mathbf{u}_s)\mathbf{u}_c = \mathbf{D}\mathbf{u}_c-\Omega\mathbf{G}_c p_c, \quad (1)$$

$$\mathbf{M}\mathbf{u}_s = \mathbf{0}_c, \quad (2)$$

where $\mathbf{u}_c\in\mathbb{R}^{3n}$ and $\mathbf{p}_c\in\mathbb{R}^n$ are the cell-centered velocity and the cell-centered pressure, respectively. The face-centered quantities, such as $\mathbf{u}_s\in\mathbb{R}^m$ are related to the cell-centered quantities via an interpolation operator $\Gamma_{c\to s}\in\mathbb{R}^{m\times 3n}$:

$$\mathbf{u}_s=\Gamma_{c\to s}\mathbf{u}_c. \quad (3)$$

Finally, $\Omega\in\mathbb{R}^{3n\times 3n}$ is a diagonal matrix containing the cell volumes, $\mathbf{C}(\mathbf{u}_s)\in\mathbb{R}^{3n\times 3n}$ is the discrete convective operator, $\mathbf{D}\in\mathbb{R}^{3n\times 3n}$ is the discrete diffusive operator, $\mathbf{G}_c\in\mathbb{R}^{3n\times n}$ is the cell-to-cell discrete gradient operator and $\mathbf{M}\in\mathbb{R}^{n\times m}$ is the face-to-cell discrete divergence operator. After applying the Fractional Step Method (FSM) to the Navier-Stokes equations, the velocity correction reads:

$$\mathbf{u}_c^{n+1}=\mathbf{u}_c^{p}-\Gamma_{s\to c}\mathbf{G}p_c^{n+1}, \quad (4)$$

where $\Gamma_{s\to c} \in \mathbb{R}^{3n\times m}$ is the face-to-cell interpolator, which is related to the cell-to-face interpolator via the volume matrices $\Gamma_{s\to c} = \Omega^{-1}\Gamma_{c\to s}\Omega_s$, and $\mathbf{G} \in \mathbb{R}^{m\times n}$ is the cell-to-face gradient operator.

Only three discrete geometrical operators are needed to formulate these equations: the cell-centered and staggered control volumes (diagonal matrices), Ω_c and Ω_s, the face normal vectors, N_s; plus two non-geometrical ones: the scalar cell-to-face interpolation, $\Pi_{c\to s}$ and the cell-to-face divergence operator, $\mathbf{M}$. For more details of these operators and its construction, the reader is referred to [3]. Due to its simplicity, these operators can be easily built in existing codes, such as OpenFOAM [4]. In contrast to a collocated arrangement, a staggered symmetry-preserving discretization can be found in [5].

2. An energy-preserving unconditionally stable FSM

From our point of view, the physical structure of the equations is only respected when the symmetries of these differential operators is preserved. For instance, constructing $\mathbf{G} = -\Omega_s\mathbf{M}^T$ is necessary to preserve kinetic energy [3], but it is also mimicking the symmetries of the continuous level operators [6].

The turbulence phenomenon is caused by a balance between convective transport and diffusive dissipation. The discrete forms of these two physical processes are defined by $\mathbf{C}(\mathbf{u}_s)$ and $\mathbf{D}$, respectively. At the continuous level, the convective operator is skew-symmetric, while the diffusive operator is symmetric and negative-definite. If we keep these properties at the discrete level (namely $\mathbf{C}(\mathbf{u}_s)$ being a skew-symmetric matrix, $\mathbf{D}$ being a symmetric negative-definite matrix and $\mathbf{G} = -\Omega_s\mathbf{M}^T$), the discrete convective operator will transport energy from resolved motion scales to others without dissipating energy.

The utility of an algebraic formulation can be found, as an example, in [1, 2]. In these works, the matrix-vector formulation is employed to investigate the stability of the solution in terms of the pressure gradient interpolation in collocated frameworks. To do so, the eigenvalues of $\mathbf{L} - \mathbf{L}_c$ were deeply studied ($\mathbf{L} = \mathbf{MG} \in \mathbb{R}^{n\times n}$ is the compact Laplacian operator whereas $\mathbf{L}_c = \mathbf{M}\Gamma_{c\to s}\Gamma_{s\to c}\mathbf{G} \in \mathbb{R}^{n\times n}$ is the collocated wide-stencil Laplacian operator), and the cell-to-face interpolation that leads to an unconditionally stable FSM turned out to be:

$$\Pi_{c\to s} = \Delta_s^{-1}\Delta_{sc}^T \in \mathbb{R}^{m\times n}, \tag{5}$$

where $\Delta_s \in \mathbb{R}^{m\times m}$ is a diagonal matrix containing the projected distances between two adjacent control volumes, and $\Delta_{sc} \in \mathbb{R}^{n\times m}$ is a matrix containing the projected distance between a cell node and its corresponding face. For details, the reader is encouraged to consult[1, 2].

3. Conservation of global kinetic energy

The global discrete kinetic energy temporal evolution equation can be obtained by left-multiplying Eq. (1) by $\mathbf{u}_c^T$ and adding it with its transpose. Taking into account that the convective operator should be skew-symmetric:

$$\frac{d}{dt}||\mathbf{u}_c||^2 \;=\; \mathbf{u}_c^T(\mathbf{D}+\mathbf{D}^T)\mathbf{u}_c - \mathbf{u}_c^T\Omega\mathbf{G}_c p_c - p_c^T\mathbf{G}_c^T\Omega^T\mathbf{u}_c. \tag{6}$$

The pressure error contribution introduced to the discrete kinetic energy equation is zero for symmetry-preserving staggered formulations, due to the fact that $\mathbf{G} = -\Omega_s\mathbf{M}^T$, and the

incompressibility constraint $\mathbf{M}\mathbf{u}_s = 0$. However, in collocated formulations $\mathbf{M}_c\mathbf{u}_c \approx 0$, but not strictly zero.

In collocated framework, the (artificial) kinetic energy added is given by:

$$-\mathbf{p}_c^T G_c^T \Omega^T \mathbf{u}_c = \mathbf{p}_c^T (\mathbf{L} - \mathbf{L}_c)\mathbf{p}_c \Delta t. \tag{7}$$

The interpolation shown in Eq. (5) assures that $\mathbf{L} - \mathbf{L}_c$ is negative definite [1, 2], so the contribution of the (artificial) kinetic energy added by the pressure term is dissipative, ensuring the stability of the simulation. However, it is important to quantify it.

4. Stability of the method

The stability of the method was confirmed using numerical tests that apply extremely coarse and very poor quality meshes. Figures 1 and 2 show an example of an air-filled ($Pr = 0.71$) differentially heated cavity with aspect ratio 2 at Rayleigh number (based on the cavity height) of 10^6, respecting operator symmetries and interpolating the pressure gradient using Eq. (5).

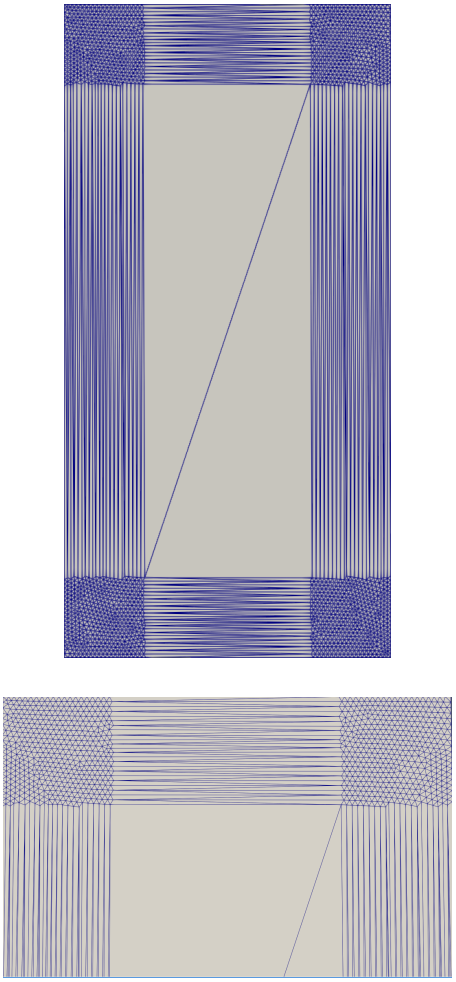

Figure 1: (Top) Test mesh used to check the stability of the method. (Bottom) Zoom at the top part of the mesh.

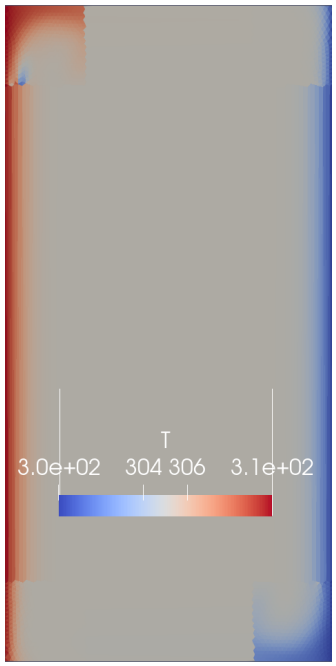

Figure 2: Temperature distribution obtained for $Ra = 10^6$ using the mesh displayed in Figure 1.

As seen in Fig. 2, the method is stable, producing results without blowing up the simulation. The accuracy will be low, as we would anticipate from such a low-quality mesh. It is worth noting that using different interpolations for the pressure gradient, such as $\frac{1}{2}$ weights will immediately blow up the simulation.

Once we assured the stability of the method, the energy budgets will be computed, in order to quantify the (artificial) contribution of the pressure term to the discrete kinetic energy, as it is done in [3].

5. Numerical test: turbulent differentially heated cavity

In this section, the accuracy of the presented discretization is tested by means of a 2D air-filled ($Pr = 0.71$) differentially heated cavity [7]. A temperature difference ΔT is found across the vertical isothermal walls, whereas the top and bottom walls are adiabatic. A height aspect ratio of $L_3/L_2 = 4$ and a Rayleigh number of $Ra = 10^{10}$ (based on the cavity height) have been chosen for the sake of comparison [3, 7]. A transport equation for the temperature T has been discretized using the same operators presented in the previous sections and the Boussinesq approximation is considered in order to take into account gravitational effects.

This case is of particular interest to test our method because, in terms of energy budgets, the dissipation rate (destruction) should counter the buoyancy effects (production). This balance between production and destruction lead us to expect the evolution of the global kinetic energy to be zero. Of course, numerical discrepancies will be found due to the chosen discretization. Furthermore, if a collocated arrengement is used, a (hopefully small) term due to the pressure gradient contribution to the kinetic energy will also be present.

Besides, three different interpolators were tested for the pressure gradient interpolation: a linear interpolation, a mid-point interpolation ($\frac{1}{2}$ weigths) and a volumetric interpolation (see eq. (5)).

5.1 Structured discretization

The first test was done using a structured mesh with $N_2 = 128$ and $N_3 = 326$, applying the following stretching to the x_2-coordinate:

$$(x_2)_k = \frac{1}{2}\frac{L_2}{L_3}(1 + \frac{tanh\{\gamma_2(2(k-1)/N_2 - 1)\}}{tanh\gamma_2}), \quad k = 1, ..., N_2 + 1. \tag{8}$$

This mesh, with an stretching factor $\gamma_2 = 2$, was proven in [7] to be sufficient to obtain accurate solutions. Figure 3 shows a zoom of the top part of this mesh. However, it is worth to mention that the time scheme used in that work is not the same that the one chosen here (the already implemented Euler time scheme in OpenFOAM).

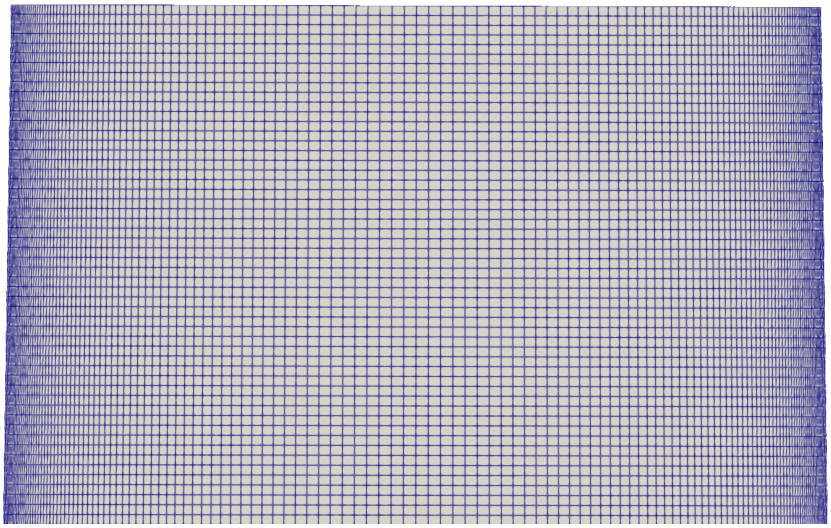

Figure 3: Top part of the mesh used to check the accuracy of the method.

A total time of $800s$ was simulated, with a $\Delta t = 0.005s$, which mantains a maximum Courant number of around 0.45 and a mean Courant number of 0.033. The average time was selected to be $400s$. The normalized time-averaged values of the contributions to the global kinetic energy can be found in table 1 for the different interpolations. They have been normalized with respect to the averaged total dissipation rate.

Interpolation	**Conv**	**Diff**	**Buoyancy**	**PressGrad**
Linear	≈ 0	-1	1.01062	-4.90×10^{-3}
Mid-point	≈ 0	-1	1.01168	-4.99×10^{-3}
Volumetric	≈ 0	-1	1.01099	-4.89×10^{-3}

Table 1: Time-averaged normalized contributions to the global kinetic energy for different pressure gradient interpolations.

As expected, the contribution of the convective term is practically zero, due to the skew-symmetric convective operator. The results are found to be very similar because in the particular case of the mesh being locally uniform (that is, low aspect ratios are found between adjacent control volumes) the three interpolators are practically the same. However, with such a mesh, small differences are present. Finally, the pressure gradient contribution is negative for the three

interpolators in this case, which was also expected. This negative contribution of the pressure gradient is assuring the method to be stable. Once this contribution becomes positive, which can be the case for the linear and mid-point interpolations in highly distorted meshes [2], energy is introduced to our system, making the simulation to blow up.

It is worth to mention that in this case, the amount of artificial kinetic energy introduced by the volumetric interpolation seems to be smaller, but very similar to the linear one. The mid-point interpolation seems to behave clearly worse than the other two.

5.2 Cartesian uniform discretization

In this section, a comparison of the previous results will be done against a better resolution mesh. To do so, a Cartesian uniform grid of $N_2 = 250$ and $N_3 = 1000$ ($N_{total}^{1/2} = 500$) was used. This number of control volumes was chosen taking into account that in [3] the results were already converged with this mesh to the selected reference solution. Furthermore, the fact that the mesh is Cartesian and uniform assures that the results are not depending on the chosen interpolation.

A total time of $800s$ was simulated, with a variable Δt, mantaining a maximum Courant number below 1 and a mean Courant number below 0.15. The average time was selected to be $400s$. The normalized time-averaged values of the contributions to the global kinetic energy can be found in table 2. They have been normalized with respect to the averaged total dissipation rate. Besides, a comparison against the previous obtained results have been done to see which results are closer to the Cartesian uniform ones. To do so, the diffusive and the buoyancy contributions of the previous results were normalized by the Cartesian uniform diffusive and buoyancy contributions, respectively.

Interpolation	**Conv**	**Diff**	**Buoyancy**	**PressGrad**
Cartesian uniform	≈ 0	-1	0.99957	-5.33×10^{-4}
Linear		0.98145	0.99230	
Mid-point		0.97782	0.98966	
Volumetric		0.98181	0.99302	

Table 2: Time-averaged normalized contributions to the global kinetic energy for the Cartesian uniform grid (row 1). Normalized comparison of the resuts obtained with the stretched meshes compared to the Cartesian uniform ones (rows $2-4$).

It can be seen that the balance obtained for the Cartesian uniform grid is closer to 1 that the previous ones. Furthermore, again it is noticeable that the mid-point interpolation works worse than the other two, while the volumetric behaves slightly better than the linear.

5.3 Unstructured discretization

Taking into account that it is always difficult to do a direct comparison between structured and unstructured grids, an unstructured triangular mesh of $N_{total}^{1/2} \approx 506$ was used. Figure 4 show the top part of this mesh:

The normalized time-averaged values of the contributions to the global kinetic energy for this particular unstructured grid can be found in table 3 for the different interpolations. Besides, a comparison with the Cartesian uniform grid results can be also found.

In this case, again, the convective contribution is almost zero and the balance between the

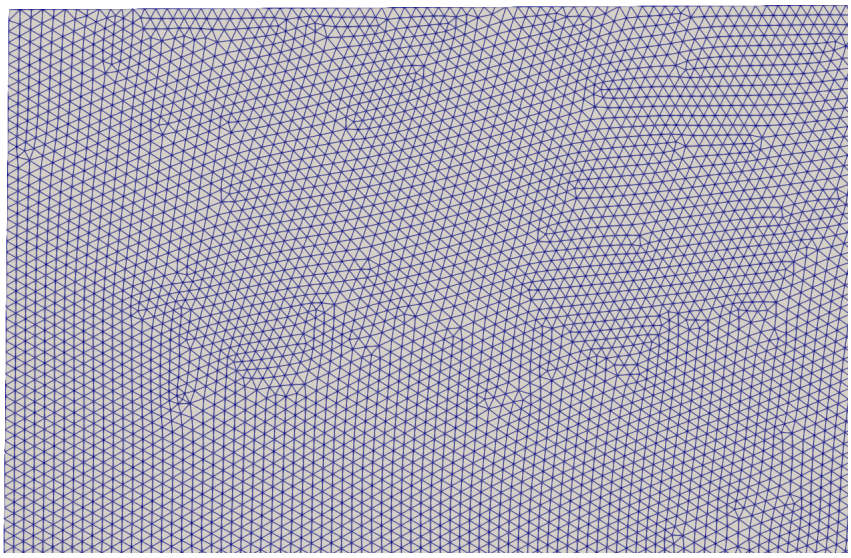

Figure 4: Top-left part of the unstructured mesh used to check the accuracy of the method.

Interpolation	**Conv**	**Diff**	**Buoyancy**	**PressGrad**
Linear	≈ 0	-1	1.00854	-1.33×10^{-3}
Mid-point	≈ 0	-1	1.00968	-1.35×10^{-3}
Volumetric	≈ 0	-1	1.01063	-1.59×10^{-3}
Linear		0.97640	0.98516	
Mid-point		0.97439	0.98424	
Volumetric		0.97840	0.98923	

Table 3: Time-averaged normalized contributions to the global kinetic energy for different pressure gradient interpolations for the unstructured mesh (rows $1-3$). Normalized comparison of the resuts obtained with the unstructured mesh compared to the Cartesian uniform ones (rows $4-6$).

production and destruction is very similar for the three interpolators. Perhaps this is due to the fact that, despite the mesh being unstructured, it is very uniform, and the presence of high aspect ratio control volumes is not found. Nonetheless, the results of the volumetric interpolation are slightly closer to the Cartesian uniform grid results than the other two.

Finally, even though the pressure gradient contribution is negative and very small in comparison, it seems that the volumetric interpolator is introducing more artificial kinetic energy than the other two. This result is totally opposite to what we found before in table 1. It is noteworthy to highlight that the centroid of the control volumes was located at the barycenter and this affects to the weights of the linear and volumetric interpolations. It would also be of interest to check if this feature is found using circumcentric centroids.

5.4 Final discussion

As it can be seen from previous sections, the mid-point interpolation seems to perform slightly worse than the linear and the volumetric ones. Despite the fact that for low-distorted meshes the linear and the volumetric seems to behave similar, when high-aspect ratio control volumes

are introduced to the grid, the linear interpolation becomes very unstable. In order to illustrate that fact, let us consider the mesh from Figure 5.

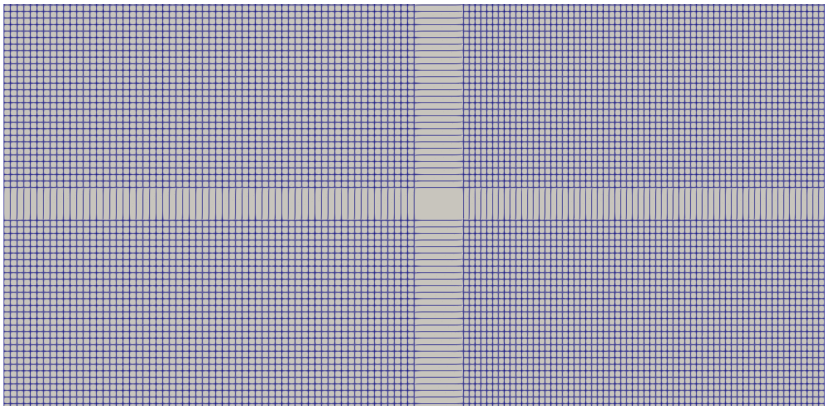

Figure 5: Central part of the 125x500 mesh used to test the stability of the linear interpolator. The maximum aspect ratio of this mesh is 6.

The maximum aspect ratio present in the mesh is 6 (between the central control volume and the adjacent ones). Perhaps this is a high aspect ratio for structured meshes, but it can be seen more often in non-structured grids. The artificial kinetic energy added up by the pressure gradient can be seen in Figure 6.

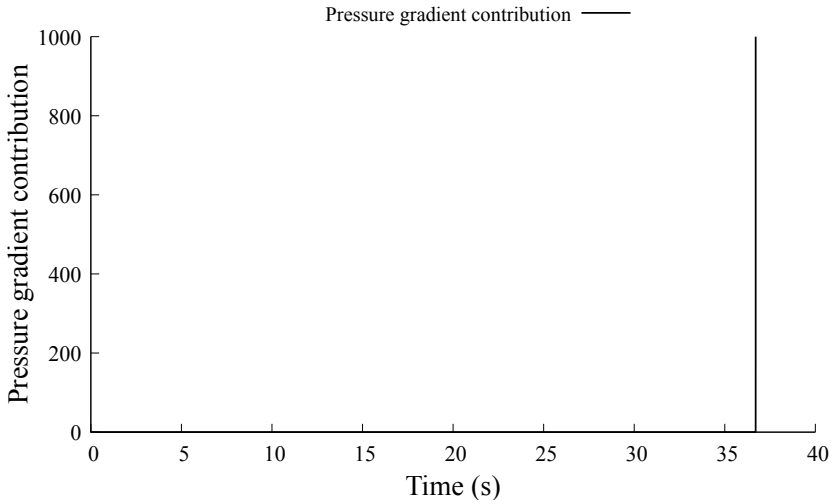

Figure 6: (Artificial) kinetic energy added up by the pressure gradien contribution as a function of time.

Figure 6 shows the point where the simulation starts to diverge (around t=37s). Until that point, the artificial kinetic energy contribution by the pressure gradient remains small and negative, but suddenly it jumps to positive values, making the simulation unstable and finally blowing it up. For the mid-point interpolator, higher aspect ratio control volumes are needed to blow up the simulation, but examples can be found in Figure 1 or in [2] for a turbulent channel flow.

Finally, a discussion of the accuracy of the mid-point interpolator and the volumetric interpolator will be done for a high-distroted mesh (see Figure 7). This mesh is not able to fully

resolve the case, but will allow a comparison between the two interpolators.

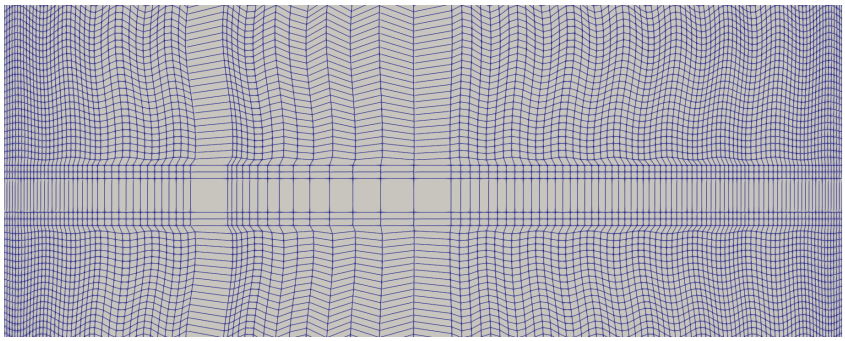

Figure 7: Central part of the high-distorted mesh used to test the accuracy of the mid-point and volumetric interpolator.

The normalized time-averaged values of the contributions to the global kinetic energy for this particular distorted grid can be found in table 4 for the different interpolations. Besides, a comparison with the Cartesian uniform grid results can be also found.

Interpolation	**Mean Δt**	**Conv**	**Diff**	**Buoyancy**	**PressGrad**	**Balance Sum**
Mid-point (maxCo=1)	0.0126	≈ 0	-1	1.97610	-0.77851	3.33×10^{-4}
Volumetric (maxCo=1)	0.0138	≈ 0	-1	1.90565	-0.93355	3.67×10^{-6}
Mid-point (fixed Δt)	0.0050	≈ 0	-1	1.57681	-0.57593	1.35×10^{-6}
Volumetric (fixed Δt)	0.0050	≈ 0	-1	1.43591	-0.43495	1.42×10^{-6}
Mid-point (maxCo=1)	0.0126		1.31246	2.59466		
Volumetric (maxCo=1)	0.0138		1.24703	2.37740		
Mid-point (fixed Δt)	0.0050		1.19875	1.89101		
Volumetric (fixed Δt)	0.0050		1.15685	1.66184		

Table 4: Time-averaged normalized contributions to the global kinetic energy for different pressure gradient interpolations for the distorted mesh (rows $1-4$). The balance sum column refers to the sum of all the non-normalized contributions. Normalized comparison of the resuts obtained with the distorted mesh compared to the Cartesian uniform ones (rows $4-8$).

For this comparison, two values of Δt have been selected. The first one, referred in table 4 as maxCo=1 is selected at each time step such as the maximum Courant number is 1, while the second selected time step is fixed ($\Delta t = 0.005$). For all the test cases, the convective term contribution was almost zero (except round-off errors), as expected for a skew-symmetric convective operator without boundary contributions. Observe that the mean Δt for the volumetric interpolator was higher than the mean Δt for the mid-point.

Even though the selected mesh is not able to fully resolve the case, the balance between the buoyancy and the diffusive term is always closer to 1 for the volumetric interpolator than for the mid-point one. For the maxCo=1 case, while the pressure gradient contribution is very high for both cases, the balance sum for the mid-point interpolator was much worse than the one obtained for the volumetric one. Remarkably is the fact that reducing the time step improves drastically the balances, and also reduces the pressure gradient contribution, as shown in Eq.(7).

Finally, when comparing the results with the ones obtained with the Cartesian uniform grid, the volumetric interpolator shows a much superior performance than the mid-point one, even with higher time steps.

6. Conclusions

An unconditionally energy-preserving fractional step method for collocated grids have been presented in this work. Within this framework, a comparison between the three classical ways to interpolate the pressure gradient have been studied: linear interpolation, mid-point interpolation and volumetric interpolation. The volumetric interpolator was shown to be unconditionally stable even for high-distorted meshes, both theoretically and numerically.

Under low-distorted meshes, the performance in accuracy of the three interpolators have been tested. While the three of them behaves similar acting in this kind of grids, it seems that the mid-point gives slightly worse results, and the volumetric gives slightly better ones. Furthermore, the linear interpolations quickly becomes unstable when the mesh is distorted. Finally, the volumetric interpolator showed a superior performance in high-distorted meshes. For this reasons, a volumetric interpolation seems to be the best option among these three to interpolate the pressure gradient.

Acknowledgements

This work has been supported by the *Ministerio de Economìa y competitividad*, Spain, RETOtwin project (PDC2021-547 120970-I00). D. Santos acknowledges a *FI AGAUR-Generalitat de Catalunya* fellowship (2022FI_B_00173).

References

1. D. Santos, J. Muela, N. Valle and F.X. Trias. On the Interpolation Problem for the Poisson Equation on Collocated Meshes. *14th WCCM-ECCOMAS Congress 2020*, July 2020 (postponed to January 2021 due to COVID19 pandemic).
2. D. Santos, F.X. Trias, G. Colomer and C.D. Pérez-Sergarra. An energy-preserving unconditionally stable fractional step method on collocated grids. *8th European Congress on Computational Methods in Applied Sciences and Engineering, ECCOMAS 2022*, Oslo, June 2022.
3. F.X. Trias, O. Lehmkuhl, A. Oliva, C.D. Pérez-Segarra, and R.W.C.P. Verstappen. Symmetry-preserving discretization of Navier-Stokes equations on collocated unstructured meshes. *Journal of Computational Physics*, 258:246–267, 2014.
4. E. Komen, J.A. Hopman, E.M.A. Frederix, F.X. Trias, and R.W.C.P. Verstappen. A symmetry-preserving second-order time-accurate PISO-based method. *Computers & Fluids*, 225:104979, 2021.
5. R.W.C.P. Verstappen, A.E.P. Veldman. Symmetry-preserving discretization of turbulent flow. *Journal of Computational Physics*, 187(1), 343-368, 2003.
6. J. J. Kreeft. Mimetic spectral element method; a discretization of geometry and physics. *Doctoral thesis*, Fac. of Aerospace Eng., TU Delft, ISBN 9789461919281
7. F.X. Trias, M. Soria, A. Oliva, C.D. Pérez-Segarra. Direct numerical simulations of two- and three-dimensional turbulent natural convection flows in a differentially

heated cavity of aspect ratio 4. *Journal of Fluid Mechanics*, 586, 259-293 (2007). doi:10.1017/S0022112007006908